PROCEEDINGS OF SCIENCE

Anisotropies in the Arrival Direction Distribution of Ultra-High Energy Cosmic Rays Measured by the Telescope Array Surface Detector

Jihyun Kim,[a,*] **Dmitri Ivanov,**[a] **Kazumasa Kawata,**[b] **Hiroyuki Sagawa**[b] **and Gordon Thomson**[a] **for the Telescope Array Collaboration**

[a] *High Energy Astrophysics Institute and Department of Physics and Astronomy, University of Utah Salt Lake City, Utah 84112-0830, USA*

[b] *Institute for Cosmic Ray Research, University of Tokyo, Kashiwa, Chiba 277-8582, Japan*

E-mail: jihyun@cosmic.utah.edu

Ultra-high energy cosmic rays (UHECRs) are extremely energetic, charged particles with energies greater than 10^{18} eV, originating from outer space. We investigate anisotropic patterns in the arrival direction distribution of UHECRs to identify their source locations. The Telescope Array (TA) experiment, the largest UHECR observatory in the northern hemisphere, has observed evidence of two intermediate-scale anisotropies in UHECR arrival direction distributions: the TA Hotspot and the Perseus-Pisces supercluster excess. In this presentation, we will describe an oversampling analysis that we performed to find the excess of events using the data measured by the TA surface detector array. We will report the latest results of the TA Hotspot and Perseus-Pisces supercluster excesses.

38th International Cosmic Ray Conference (ICRC2023)
26 July - 3 August, 2023
Nagoya, Japan

*Speaker

PoS(ICRC2023)244

1. Introduction

Ultra-high energy cosmic rays (UHECRs) are extremely energetic, charged particles with energies greater than 10^{18} eV, originating from outer space. The origin of these particles has been a subject of research for a long time; however, it remains a crucial question yet to be answered due to the presence of cosmic magnetic fields that deflect their trajectories. Nonetheless, by studying the arrival direction distribution of cosmic rays with energies greater than $10^{19.5}$ eV, it may be possible to identify their source locations since they are expected to experience only small deflections. An analysis of the anisotropy of the arrival direction distribution can reveal characteristic distributions that may provide indications of UHECR source locations.

The first report of the intermediate-scale anisotropy in the arrival direction distribution of UHECR events measured by the Telescope Array (TA) experiment was a high concentration of events with energies greater than 5.7×10^{19} eV, the so-called TA Hotspot [1]. It was observed near the direction of the Ursa Major constellation using a total of 72 events observed by the surface detector array over a 5-year period. By performing an oversampling analysis with 20°-radius circles, we obtained a 5.1σ excess of events compared to isotropic backgrounds using the Li-Ma method, described in Section 3.2. The chance probability of detecting a hotspot with Li-Ma significance equal or greater than the data in an isotropic sky was calculated to be 3.7×10^{-4} (3.4σ) assuming 15°, 20°, 25°, 30°, and 35° oversampling radius circle searches.

However, no notable potential sources corresponding to the direction of the Hotspot have been identified within the observable distance range of UHECR events, ~100 Mpc, taking into account a theoretical upper limit on the energy of cosmic ray protons traveling from their sources. Numerous studies have explored potential sources of the TA Hotspot, such as M82, Mrk 180 [2], Mrk 421 [3], and filaments of galaxies connected to the Virgo cluster [4]. Despite these efforts, the source of the Hotspot remains undetermined. Since the first report, we have constantly updated the Hotspot measurements with new data, and the Hotspot persists in TA data with over $\sim 3\sigma$ significance [5].

Recently, while studying the energy spectrum mismatch in the TA and Auger data, we observed a new intermediate-scale anisotropy in the arrival direction distributions of events at slightly lower energies than the TA Hotspot energy [5, 6]. We made sky maps of events with minimum energy thresholds of $10^{19.4}$ eV, $10^{19.5}$ eV, and $10^{19.6}$ eV, where the energy spectrum excess becomes prominent, and found an intermediate scale anisotropy appearing in the direction of the Perseus-Pisces supercluster (PPSC) for each energy range. We used 11 years of data recorded by the surface detector array that had 864, 558, and 335 events with minimum energy thresholds of $10^{19.4}$ eV, $10^{19.5}$ eV, and $10^{19.6}$ eV, respectively. With 20°-radius circles, we obtained Li-Ma significances of 4.4σ, 4.2σ, and 4.0σ for the three energy ranges [6].

Since the new excess of events appears in the region of the PPSC, which is one of the notable structures within TA's field of view, we estimated the chance probabilities that random excesses could be observed as close to the PPSC as data in isotropic skies of UHECRs. Two criteria, the maximum Li-Ma significance and its angular distance to the center of the PPSC, were used for assessing Monte Carlo simulations. The chance probabilities of excesses appearing in the Monte Carlo trials, with sigmas greater than or equal to that of the data, and as close to the PPSC as the data, were estimated to be 3.6σ, 3.6σ, and 3.4σ for the three energies, respectively.

In this work, we report on the intermediate-scale anisotropies, the TA Hotspot and the PPSC excess, measured by the Telescope Array experiment using the most up-to-date data, collected over

15 years.

2. Telescope Array Experiment

The Telescope Array (TA) experiment is the largest UHECR observatory in the northern hemisphere. It employs a hybrid technique to observe extensive air showers induced by primary ultra-high energy particles striking the Earth's atmosphere. The observatory is located in the west desert of Utah, USA (39.3° N, 112.9° W, 1400 m above sea level). A total of 507 surface detectors (SDs) are spread out with 1.2 km spacing on a square grid over approximately 700 km^2 area to measure the air showers induced by UHECRs. Each SD counter has two layers of plastic scintillator to sample the footprint of the extensive air shower when it reaches ground level [7]. Three fluorescence detector (FD) stations are sited at the apices of a triangle with each station having a field of view overlooking the area of the SD array. A total of 38 fluorescence telescopes in the FD stations measure the ultraviolet light emitted as the extensive air shower traverses the atmosphere, viewing 3°–31° in elevation [8].

3. Methods

3.1 Event Selection

To investigate intermediate-scale anisotropies in the arrival direction distributions, we use 15 years of TA data recorded between May 11, 2008, and May 10, 2023, by the surface detector array. We have two analyses for the intermediate-scale anisotropies. The main difference lies in their energy thresholds. The TA Hotspot analysis, which was the first anisotropy observed in TA data, uses the minimum energy of 5.7×10^{19} eV, whereas for the PPSC excess one adopts a threshold of $10^{19.4}$ eV, where an excess in the energy spectrum was observed. In addition to this, the details of the selection criteria are slightly different to include a sufficient number of events while keeping reasonable energy and angular resolutions.

The selection criteria adopted for the PPSC excess are as follows:

1. Each event must include at least five SD counters.
2. The reconstructed primary zenith angle must be less than 55°.
3. Both the geometry and lateral distribution fits must have χ^2/degree of freedom less than 4.
4. The angular uncertainty estimated by the geometry fit must be less than 5°.
5. The fractional uncertainty in S800 estimated by the lateral distribution fit must be less than 25%.
6. The counter with the largest signal must be surrounded by four working counters: one to the north, east, south, and west on the grid, but they do not have to be immediate neighbors of the largest signal counter.

The ongoing TA Hotspot analysis employs the same energy threshold and selection criteria as those utilized in the original Hotspot paper [1] to keep the consistency of the analysis. In the original Hotspot paper, we used TA SD data collected over 5 years; therefore, it was necessary to introduce slightly looser selection criteria than those described above to include a sufficient number of high energy events while keeping reasonable energy and angular resolutions. The main differences are described as follows:

1. Each event includes at least four SD counters.
2. The angular uncertainty estimated by the geometry fit must be less than 10°.

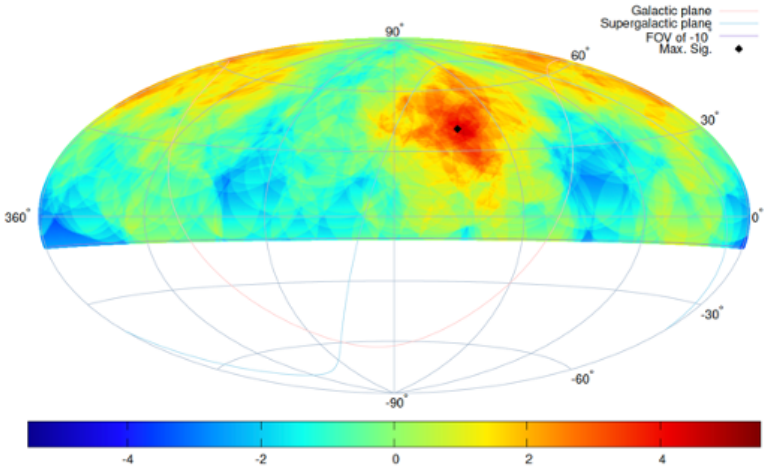

Figure 1: The sky map of the TA Hotspot in equatorial coordinates using a Hammer projection. Color represents the Li-Ma significance using a 25°-radius circle angular window in equatorial coordinates for 15 years of SD events with $E > 5.7 \times 10^{19}$ eV. The black diamond indicates the maximum Li-Ma significance position at (144.0°, 40.5°). The color code indicates an excess (red) and a deficit (blue) of events compared to isotropy.

The energy scale of the SD was normalized to match the FD calorimetric energy scale using hybrid events [9]. Using these event selection criteria, 1125 events remain with $E > 10^{19.4}$ eV for the PPSC excess analysis and 216 events with $E > 5.7 \times 10^{19}$ eV for the Hotspot analysis in the 15-year data set. The energy and angular resolutions of this data set are 20% and 1.5°, respectively.

3.2 Oversampling Analysis

To investigate anisotropies in the arrival direction distributions, we perform oversampling searches using intermediate-scale angular circles and estimate the significances of excesses or deficits of events compared to the isotropic background events by Monte Carlo simulations [10]:

$$S_{\mathrm{LM}} = \sqrt{2}\left[N_{\mathrm{on}} \ln\left(\frac{(1+\alpha)N_{\mathrm{on}}}{\alpha(N_{\mathrm{on}}+N_{\mathrm{off}})}\right) + N_{\mathrm{off}} \ln\left(\frac{(1+\alpha)N_{\mathrm{off}}}{N_{\mathrm{on}}+N_{\mathrm{off}}}\right)\right]^{1/2}. \quad (1)$$

First at each grid point in right ascension (0°–360°) and declination (−10°–90°), using 0.1° steps, we count the number of events within a given angular scale circle for the data, defined as N_{on}. Then, the number of events outside the circle is determined by subtraction from the total number of events, $N_{\mathrm{off}} = N_{\mathrm{tot}} - N_{\mathrm{on}}$. Next, the same calculation at each grid point is conducted for an isotropic simulation to determine the exposure ratio of **on** to **off**, $\alpha = N_{\mathrm{iso,on}}/N_{\mathrm{iso,off}}$. In this analysis, we used 10^5 events assuming an isotropic flux taking into account the TA's geometrical exposure $g(\theta) = \sin\theta\cos\theta$ as a function of zenith angle (θ) because the detection efficiency for this energy range is ∼100% regardless of zenith angle θ.

4. Results and Discussion

4.1 Telescope Array Hotspot

In this analysis, we use 15 years of data, collected by the Telescope Array surface detector array, with the same energy threshold, 5.7×10^{19} eV, adopted in the initial report. A total of 216

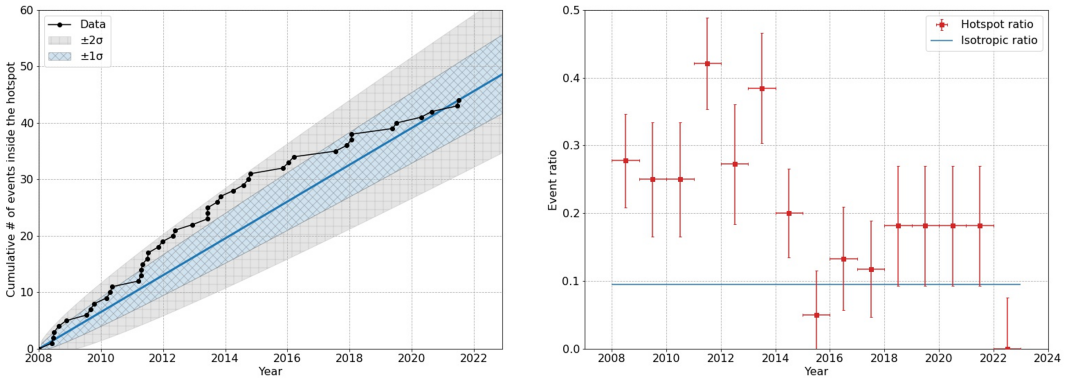

Figure 2: The growth and event ratio of the TA Hotspot. (Left) The black dots show the cumulative number of events falling inside the Hotspot circle with a radius of 25° centered at (144.0°, 40.5°). The blue solid line indicates the estimated event rate inside the Hotspot. The light blue and gray bands show $\pm 1\sigma$ and $\pm 2\sigma$ deviations from a linear increase rate. **(Right)** The red dots indicate the event ratio: the number of events falling inside the Hotspot to the total number of events with energy greater than 5.7×10^{19} eV. The blue solid line represents the event ratio of the number of isotropic simulation events falling inside the Hotspot region to their total number of events.

events are in this data set. Note, however, in the initial report a 20°-radius oversampling circle was used. We now use 25°-radius circles for the oversampling analysis.

Performing an oversampling analysis with 25°-radius circles, the maximum Li-Ma significance is calculated to be 4.8σ at the position of (144.0°, 40.5°) in equatorial coordinates. At the position of maximum Li-Ma significance, it is observed that 44 out of 216 events are located within a 25°-radius circle, whereas 18.0 events are expected from an isotropic distribution. Figure 1 shows the sky map of the TA Hotspot in equatorial coordinates using a Hammer projection. The black diamond indicates the position of maximum Li-Ma significance (144.0°, 40.5°).

To quantify how often such an excess appears anywhere in an isotropic UHECR sky within TA's field of view by chance, we generate many Monte Carlo event sets. Each Monte Carlo set contains the same number of events as the data (216 events), thrown isotropically taking into account the geometrical exposure of the TA surface detector array. We count as successes the number of sets where the maximum Li-Ma significance is at least as significant as the data, ($S_{\rm MC} > S_{\rm obs}$). The chance probability of finding such an excess is estimated to be 2.7×10^{-3}, $\sim 2.8\sigma$.

Figure 2 shows the growth of the number of events inside the Hotspot and the ratio of the number of events inside the Hotspot to the total number of events as a function of the year. The left panel shows the cumulative number of events falling inside the Hotspot circle of 25° from (144.0°, 40.5°) with black dots. We overlay the blue solid line indicating the estimated event rate inside the Hotspot. The light blue and gray bands represent $\pm 1\sigma$ and $\pm 2\sigma$ deviations from the linear increase rate. The rate of event accumulation inside the Hotspot circle is consistent with the linear growth within $\sim 2\sigma$.

The right panel of Figure 2 shows the event ratio of the TA Hotspot as a function of the year. The red points represent the ratio of the number of events falling inside the Hotspot to the total

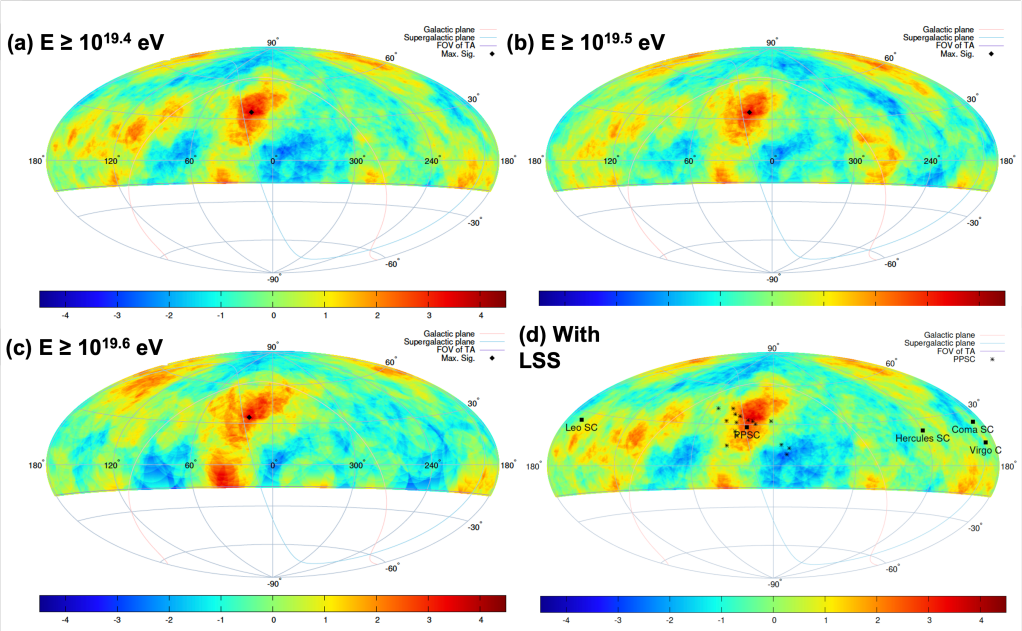

Figure 3: The sky maps of the PPSC excess in the equatorial coordinates using a Hammer projection. The Li-Ma significance maps are shown, using a 20°-circle angular windows in equatorial coordinates for different energy thresholds: (a) $E \geq 10^{19.4}$ eV, (b) $E \geq 10^{19.5}$ eV, and (c) $E \geq 10^{19.6}$ eV. Panel (d) shows the prominent structures of the local large-scale structure of the universe in TA's field of view within 150 Mpc overlaid with the significance map of $E \geq 10^{19.4}$ eV. The black squares indicate the center positions of those local large-scale structures. The black diamonds represent the positions of the maximum Li-Ma significances. The black x's indicate the locations of the brighter objects within the PPSC. The color code indicates an excess (red) and a deficit (blue) of events compared to isotropy.

number of events each year. The blue solid line represents the expected event ratio for an isotropic simulation.

Every year we thoroughly examine our newly observed data sets and have found no serious defects to affect the acceptance of the highest energy events. We conclude that there are considerable fluctuations in these data. It is necessary to continue observation to investigate the TA Hotspot feature.

4.2 Perseus-Pisces Supercluster Excess

The number of events in the 15-year TA SD data set with $E \geq 10^{19.4}$ eV, $E \geq 10^{19.5}$ eV, and $E \geq 10^{19.6}$ eV is 1125, 728, and 441, respectively. We calculate the Li-Ma significances of excess/deficit of events compared to isotropic expectations at each grid point using 20°-radius oversampling circles. Analysis results are depicted in Figure 3. The black diamonds indicate the Li-Ma significances of 4.0σ at the position of (17.9°, 35.2°) for $E \geq 10^{19.4}$ eV, 3.9σ at the position of (19.0°, 35.1°) for $E \geq 10^{19.5}$ eV, and 3.5σ at the position of (19.7°, 34.6°) for $E \geq 10^{19.6}$ eV. As seen in Fig. 4(d) the excess is coincident with the overall distribution of the elements of the PPSC. Therefore, we calculate the angular distances between the center of the PPSC and positions of the maximum of Li-Ma significance. They are 7.7°, 7.4°, and 6.8° for $E \geq 10^{19.4}$ eV, $E \geq 10^{19.5}$ eV, and $E \geq 10^{19.6}$ eV data sets. This suggests that the excess in the data is coincident with the PPSC.

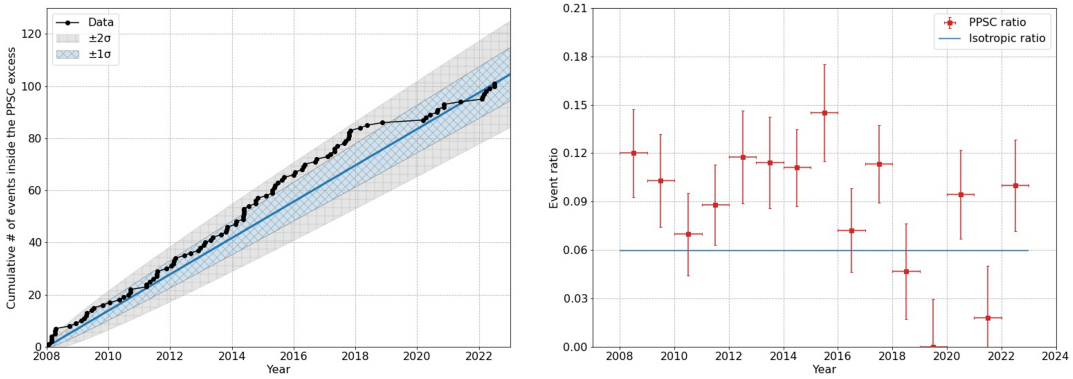

Figure 4: The growth and event ratio of the Perseus-Pisces supercluster (PPSC) excess. (Left) The cumulative number of events with $E \geq 10^{19.4}$ eV falling inside the PPSC excess circle with a radius of 20° from (17.9°, 35.2°) is shown with black dots. The blue solid line indicates the estimated event rate inside the PPSC excess. The light blue and gray bands represent $\pm 1\sigma$ and $\pm 2\sigma$ deviations from the linear increase rate, respectively. **(Right)** The red dots indicate the event ratio: the number of events falling inside the PPSC excess circle to the total number of events with $E \geq 10^{19.4}$. The blue solid line represents the event ratio of isotropic simulation events (those falling inside the PPSC excess region divided by their total number of events).

We estimate the probability of such an excess appearing in an isotropic UHECR sky by chance. For the Hotspot analysis, we applied one criterion to test whether isotropic Monte Carlo sets would be at least as significant as the data, ($S_{\rm MC} \geq S_{\rm obs}$). To estimate PPSC excess, we add one more criterion: the positions of the maximum Li-Ma significances of Monte Carlo sets should be as close to the PPSC as the data ($\theta_{\rm MC} \leq \theta_{\rm obs}$). The chance probabilities of having equal or higher excess as close to the PPSC as data are estimated to be 3.3σ, 3.2σ, and 3.0σ for $E \geq 10^{19.4}$ eV, $E \geq 10^{19.5}$ eV, and $E \geq 10^{19.6}$ eV data sets, respectively.

We examined whether there is an additional excess near any of the local large-scale structures of the universe akin to the PPSC. The structures similar to the PPSC in TA's field of view within 150 Mpc are: the Virgo cluster (17 Mpc), PPSC (70 Mpc), Coma supercluster (90 Mpc), Leo supercluster (135 Mpc), and Hercules supercluster (135 Mpc). Their center positions are marked in the Li-Ma significance map of $E \geq 10^{19.4}$ eV in Figure 3 (d). The data do not show an excess at any of the locations of other nearby major structures other than the PPSC.

This finding suggests the presence of a potential cosmic ray source in the direction of PPSC. The PPSC is of particular importance within the TA's observation range due to its distance and uniqueness. It is the closest supercluster to us, aside from the Local supercluster in which we reside. Additionally, it is next to the Local Void [11–13] where the magnetic field strength, presumed to be comparatively weaker than in other cosmic web structures, the large-scale structure of the universe, further enhances its significance. Assuming UHECR particles are ejected from the PPSC, their trajectory from the PPSC to us would be less deflected by the cosmic magnetic fields in the Local Void so that the excess of events could be measured close to the PPSC.

We also examine the growth and the event ratio of the PPSC, which are shown in Figure 4.

The increase rate of the events inside the PPSC excess circle is consistent with the linear increase within $\sim 2\sigma$. We have observed higher event ratios of the PPSC excess compared to the isotropic expectation throughout most of the observation periods with some statistical fluctuations. It is crucial to further investigate astronomical objects within the Perseus-Pisces supercluster and to increase the statistical power of northern hemisphere cosmic ray studies.

5. Summary

We investigated intermediate-scale anisotropies in 15 years of TA SD data. We have persistent evidence for the TA Hotspot at the highest energies, 5.7×10^{19} eV. The global significance of such an excess appearing by chance anywhere in TA's field of view is estimated to be 2.8σ. A new excess of events with $E \geq 10^{19.4}$ eV, slightly lower than the Hotspot, has been constantly observed in the direction of the Perseus-Pisces supercluster. The chance probability of having an equal or higher excess as close to the PPSC as data is estimated to be 3.3σ. The completion of TA×4, the four-fold expansion of the Telescope Array experiment [14], and the ongoing operation of TA are expected to play a vital role in resolving the enigma surrounding the origin of UHECRs.

References

[1] R.U. Abbasi *et al.*, *Astrophysical Journal Letters*, **790**, L21 (2014).

[2] H.-N. He *et al.*, *Physical Review D*, **93**, 043011 (2016).

[3] K. Fang, T. Fujii, T. Linden, and A.V. Olinto, *Astrophysical Journal* **794**, 126 (2014).

[4] J. Kim, D. Ryu, H. Kang, S. Kim, and S.-C. Rey, *Science Advances* **5** eaau8227, (2019).

[5] J. Kim, D. Ivanov, K. Kawata, H. Sagawa, and G. Thomson, *PoS(ICRC2021)328* (2021).

[6] R.U. Abbasi *et al.*, [arXiv:2110.14827 (2021)].

[7] T. Abu-Zayyad *et al.*, *Nuclear Instruments and Methods in Physics Research Section A-Accelerators Spectrometers Detectors and Associated Equipment*, **689**, 87 (2012).

[8] H. Tokuno *et al.*, *Nuclear Instruments and Methods in Physics Research Section A-Accelerators Spectrometers Detectors and Associated Equipment*, **676**, 54 (2012).

[9] T. Abu-Zayyad *et al.*, *Astrophysical Journal Letters*, **768**, L1 (2013).

[10] T.-P. Li and Y.-Q. Ma, *Astrophysical Journal Letters*, **272**, 317 (1983).

[11] M.P. Haynes and R. Giovanelli, *Astrophysical Journal* **306**, L55 (1986).

[12] H.M. Courtois, *et al.*, *Astronomical Journal*, **146**, 69 (2013).

[13] R.B. Tully *et al.*, *Astrophysical Journal*, **880**, 24 (2019).

[14] R.U. Abbasi *et al.*, *Nuclear Instruments and Methods in Physics Research Section A-Accelerators Spectrometers Detectors and Associated Equipment*, **1019**, 165726 (2021).

Full Authors List: Telescope Array Collaboration

R.U. Abbasi[1], Y. Abe[2], T. Abu-Zayyad[1,3], M. Allen[3], Y. Arai[4], R. Arimura[4], E. Barcikowski[3], J.W. Belz[3], D.R. Bergman[3], S.A. Blake[3], I. Buckland[3], B.G. Cheon[5], M. Chikawa[6], A. Fedynitch[6,7], T. Fujii[4,8], K. Fujisue[6], K. Fujita[6], R. Fujiwara[4], M. Fukushima[6], G. Furlich[3], Z. Gerber[3], N. Globus[9*], W. Hanlon[3], N. Hayashida[10], H. He[9], R. Hibi[2], K. Hibino[10], R. Higuchi[9], K. Honda[11], D. Ikeda[10], N. Inoue[12], T. Ishii[11], H. Ito[9], D. Ivanov[3], A. Iwasaki[4], H.M. Jeong[13], S. Jeong[13], C.C.H. Jui[3], K. Kadota[14], F. Kakimoto[10], O. Kalashev[15], K. Kasahara[16], S. Kasami[17], S. Kawakami[4], K. Kawata[6], I. Kharuk[15], E. Kido[9], H.B. Kim[5], J.H. Kim[3], J.H. Kim[3†], S.W. Kim[13], Y. Kimura[4], I. Komae[4], K. Komori[17], Y. Kusumori[17], M. Kuznetsov[15,18], Y.J. Kwon[19], K.H. Lee[5], M.J. Lee[13], B. Lubsandorzhiev[15], J.P. Lundquist[3,20], T. Matsuyama[4], J.A. Matthews[3], J.N. Matthews[3], R. Mayta[4], K. Miyashita[2], K. Mizuno[2], M. Mori[17], M. Murakami[17], I. Myers[3], S. Nagataki[9], K. Nakai[4], T. Nakamura[21], E. Nishio[17], T. Nonaka[6], S. Ogio[6], H. Ohoka[6], N. Okazaki[6], Y. Oku[17], T. Okuda[22], Y. Omura[4], M. Onishi[6], M. Ono[9], A. Oshima[23], H. Oshima[6], S. Ozawa[24], I.H. Park[13], K.Y. Park[5], M. Potts[3‡], M.S. Pshirkov[15,25], J. Remington[3], D.C. Rodriguez[3], C. Rott[3,13], G.I. Rubtsov[15], D. Ryu[26], H. Sagawa[6], R. Saito[2], N. Sakaki[6], T. Sako[6], N. Sakurai[4], D. Sato[2], K. Sato[4], S. Sato[17], K. Sekino[6], P.D. Shah[3], N. Shibata[17], T. Shibata[6], J. Shikita[4], H. Shimodaira[6], B.K. Shin[26], H.S. Shin[6], D. Shinto[17], J.D. Smith[3], P. Sokolsky[3], B.T. Stokes[3], T.A. Stroman[3], Y. Takagi[17], K. Takahashi[6], M. Takamura[27], M. Takeda[6], R. Takeishi[6], A. Taketa[28], M. Takita[6], Y. Tameda[17], K. Tanaka[29], M. Tanaka[30], S.B. Thomas[3], G.B. Thomson[3], P. Tinyakov[15,18], I. Tkachev[15], H. Tokuno[31], T. Tomida[2], S. Troitsky[15], R. Tsuda[4], Y. Tsunesada[4,8], S. Udo[10], F. Urban[32], I.A. Vaiman[15], D. Warren[9], T. Wong[3], K. Yamazaki[23], K. Yashiro[27], F. Yoshida[17], Y. Zhezher[6,15], and Z. Zundel[3]

[1] Department of Physics, Loyola University Chicago, Chicago, Illinois 60660, USA

[2] Academic Assembly School of Science and Technology Institute of Engineering, Shinshu University, Nagano, Nagano 380-8554, Japan

[3] High Energy Astrophysics Institute and Department of Physics and Astronomy, University of Utah, Salt Lake City, Utah 84112-0830, USA

[4] Graduate School of Science, Osaka Metropolitan University, Sugimoto, Sumiyoshi, Osaka 558-8585, Japan

[5] Department of Physics and The Research Institute of Natural Science, Hanyang University, Seongdong-gu, Seoul 426-791, Korea

[6] Institute for Cosmic Ray Research, University of Tokyo, Kashiwa, Chiba 277-8582, Japan

[7] Institute of Physics, Academia Sinica, Taipei City 115201, Taiwan

[8] Nambu Yoichiro Institute of Theoretical and Experimental Physics, Osaka Metropolitan University, Sugimoto, Sumiyoshi, Osaka 558-8585, Japan

[9] Astrophysical Big Bang Laboratory, RIKEN, Wako, Saitama 351-0198, Japan

[10] Faculty of Engineering, Kanagawa University, Yokohama, Kanagawa 221-8686, Japan

[11] Interdisciplinary Graduate School of Medicine and Engineering, University of Yamanashi, Kofu, Yamanashi 400-8511, Japan

[12] The Graduate School of Science and Engineering, Saitama University, Saitama, Saitama 338-8570, Japan

[13] Department of Physics, SungKyunKwan University, Jang-an-gu, Suwon 16419, Korea

[14] Department of Physics, Tokyo City University, Setagaya-ku, Tokyo 158-8557, Japan

[15] Institute for Nuclear Research of the Russian Academy of Sciences, Moscow 117312, Russia

[16] Faculty of Systems Engineering and Science, Shibaura Institute of Technology, Minato-ku, Tokyo 337-8570, Japan

[17] Graduate School of Engineering, Osaka Electro-Communication University, Neyagawa-shi, Osaka 572-8530, Japan

[18] Service de Physique Théorique, Université Libre de Bruxelles, Brussels 1050, Belgium

[19] Department of Physics, Yonsei University, Seodaemun-gu, Seoul 120-749, Korea

[20] Center for Astrophysics and Cosmology, University of Nova Gorica, Nova Gorica 5297, Slovenia

[21] Faculty of Science, Kochi University, Kochi, Kochi 780-8520, Japan

[22] Department of Physical Sciences, Ritsumeikan University, Kusatsu, Shiga 525-8577, Japan

[23] College of Science and Engineering, Chubu University, Kasugai, Aichi 487-8501, Japan

[24] Quantum ICT Advanced Development Center, National Institute for Information and Communications Technology, Koganei, Tokyo 184-8795, Japan

[25] Sternberg Astronomical Institute, Moscow M.V. Lomonosov State University, Moscow 119991, Russia

[26] Department of Physics, School of Natural Sciences, Ulsan National Institute of Science and Technology, UNIST-gil, Ulsan 689-798, Korea

[27] Department of Physics, Tokyo University of Science, Noda, Chiba 162-8601, Japan

[28] Earthquake Research Institute, University of Tokyo, Bunkyo-ku, Tokyo 277-8582, Japan

[29] Graduate School of Information Sciences, Hiroshima City University, Hiroshima, Hiroshima 731-3194, Japan

[30] Institute of Particle and Nuclear Studies, KEK, Tsukuba, Ibaraki 305-0801, Japan
[31] Graduate School of Science and Engineering, Tokyo Institute of Technology, Meguro, Tokyo 152-8550, Japan
[32] CEICO, Institute of Physics, Czech Academy of Sciences, Prague 182 21, Czech Republic

Acknowledgements

The Telescope Array experiment is supported by the Japan Society for the Promotion of Science(JSPS) through Grants-in-Aid for Priority Area 431, for Specially Promoted Research JP21000002, for Scientific Research (S) JP19104006, for Specially Promoted Research JP15H05693, for Scientific Research (S) JP19H05607, for Scientific Research (S) JP15H05741, for Science Research (A) JP18H03705, for Young Scientists (A) JPH26707011, and for Fostering Joint International Research (B) JP19KK0074, by the joint research program of the Institute for Cosmic Ray Research (ICRR), The University of Tokyo; by the Pioneering Program of RIKEN for the Evolution of Matter in the Universe (r-EMU); by the U.S. National Science Foundation awards PHY-1806797, PHY-2012934, PHY-2112904, PHY-2209583, and PHY-2209584 as well as AGS-1613260, AGS-1844306, and AGS-2112709; by the National Research Foundation of Korea (2017K1A4A3015188, 2020R1A2C1008230, & 2020R1A2C2102800); by the Ministry of Science and Higher Education of the Russian Federation under the contract 075-15-2020-778, IISN project No. 4.4501.18, by the Belgian Science Policy under IUAP VII/37 (ULB), by National Science Centre in Poland grant 2020/37/B/ST9/01821. This work was partially supported by the grants of the joint research program of the Institute for Space-Earth Environmental Research, Nagoya University and Inter-University Research Program of the Institute for Cosmic Ray Research of the University of Tokyo. The foundations of Dr. Ezekiel R. and Edna Wattis Dumke, Willard L. Eccles, and George S. and Dolores Doré Eccles all helped with generous donations. The State of Utah supported the project through its Economic Development Board, and the University of Utah through the Office of the Vice President for Research. The experimental site became available through the cooperation of the Utah School and Institutional Trust Lands Administration (SITLA), U.S. Bureau of Land Management (BLM), and the U.S. Air Force. We appreciate the assistance of the State of Utah and Fillmore offices of the BLM in crafting the Plan of Development for the site. We thank Patrick A. Shea who assisted the collaboration with much valuable advice and provided support for the collaboration's efforts. The people and the officials of Millard County, Utah have been a source of steadfast and warm support for our work which we greatly appreciate. We are indebted to the Millard County Road Department for their efforts to maintain and clear the roads which get us to our sites. We gratefully acknowledge the contribution from the technical staffs of our home institutions. An allocation of computing resources from the Center for High Performance Computing at the University of Utah as well as the Academia Sinica Grid Computing Center (ASGC) is gratefully acknowledged.

* Presently at: University of California - Santa Cruz
† Presently at: Argonne National Laboratory, Physics Division, Lemont, Illinois 60439,USA
‡ Presently at: Georgia Institute of Technology, Physics Department, Atlanta, Geogia 30332,USA